http://dx.doi.org/10.21611/qirt.2006.010

Defect Quantification with Thermographic Signal Reconstruction and Artificial Neural Networks

By Hernan Benitez*, Clemente Ibarra-Castanedo**, Humberto Loaiza*, Eduardo Caicedo*, Abdelhakim Bendada**, Xavier Maldague**

**Universidad del Valle, Colombia*
***Université Laval, Québec*

Abstract

Thermographic Signal Reconstruction (TSR) is a processing technique in Themography for Nondestructive Testing (TNDT). It is based on a least square fit of a low order polynomial to the logarithmic time evolution of experimental data. Even though TSR allows the reduction of data for processing and the filtering of high frequency noise, the resulting TSR polynomial coefficients lack of physical meaning to provide quantitative results and further processing is required in order to characterize internal defects. We propose to use Artificial Neural Networks (ANN) as a tool to map between TSR coefficients and defect depths. This paper presents the application of ANN and TSR coefficients as learning and validation data sets to characterize defects in composite materials.

1. Introduction

Thermographic Signal Reconstruction (TSR) is a processing technique that makes use of the one dimensional heat diffusion equation describing the surface temperature evolution in a semi-infinite sample after it has been thermally stimulated with a Dirac pulse [1]:

$$T = \frac{Q}{e\sqrt{\pi t}} \quad (1)$$

where *t* is the time, *e* is the material effusivity and *Q* is the energy density at the surface. This relationship can be rewritten in a double logarithmic form so that the time dependency of temperature at each pixel can be approximated with a polynomial having the following form [2]:

$$\ln[T(t)] = a_0 + a_1 \ln(t) + a_2 \ln^2(t) + ... + a_n \ln^n(t) \quad (2)$$

TSR provides good qualitative results [3] allowing the detection of defects, the reduction of data for processing and the filtration of high frequency noise. Further processing of TSR results can also be used for quantitative characterization since the logarithmic behaviours of the pixels that correspond to a defective area depart from the pseudo-linear behaviour (with slope -0.5) at a particular time that is correlated to the depth of the defect (Figures 1 and 3).

http://dx.doi.org/10.21611/qirt.2006.010

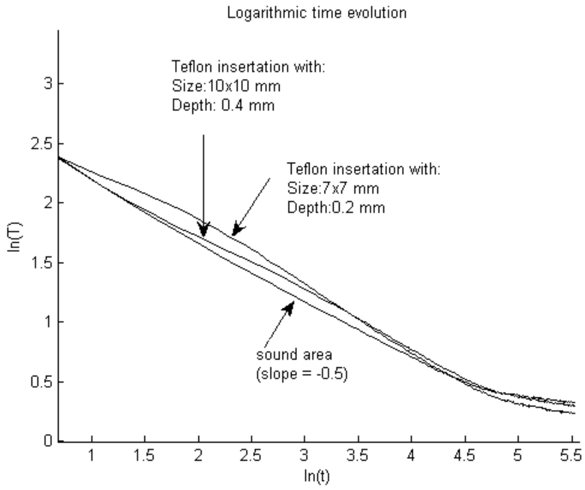

Fig. 1. *Temperature versus time evolution in a composite (CFRP) sample with Teflon® insertions with different sizes at different depths*

Although TSR generates filtered experimental data it is also worth noting that the first and second time derivatives of the filtered data have proven to be useful for quantitative purposes [4, 5] since contrast between defective and sound areas is enhanced. On the other hand, the TSR polynomial coefficients in Eq (2) allow a simple mathematical representation and a significant compression of experimental data but they lack of physical meaning that can be used for quantitative purposes. ANN are known by their ability to perform a non linear mapping between two sets of variables [6], their low sensitivity to noise and capabilities for learning and generalization [7, 8, 9,10].
The purpose of this article is to investigate the ability of ANN to map between the TSR coefficients and defect depths mathematical spaces. First, we analyse the behaviour of TSR coefficients with respect to defect depths in order to determine which coefficients are more significant for a correct mapping. Second, we train and validate several Multilayer Perceptron (MLP) architectures with TSR coefficients extracted from thermogram sequences of a CFRP sample. Finally, the results are analysed to determine the advantages and limitations of this technique.

2. TSR polynomial coefficients

TSR polynomial coefficients allow a significant degree of compression since if the entire sequence of TSR images is to be stored, it is only necessary to save the polynomial coefficients images, regardless of the length of the image sequence. In addition, coefficient images show already significant contrast improvement with respect to raw data [11]. However, TSR coefficients do not have physical meaning that allows a direct interpretation for defect characterization.
In order to use the TSR coefficients as input data to ANN and perform defect quantification, their behavior with respect to defect depth variations need to be analyzed. The aim is to determine which are the coefficients that preserve as much of the relevant information as possible and know if there is any set of input patterns

http://dx.doi.org/10.21611/qirt.2006.010

(TSR coefficients) that produces the same output patterns (defect depth) and could mislead ANN depth estimation.

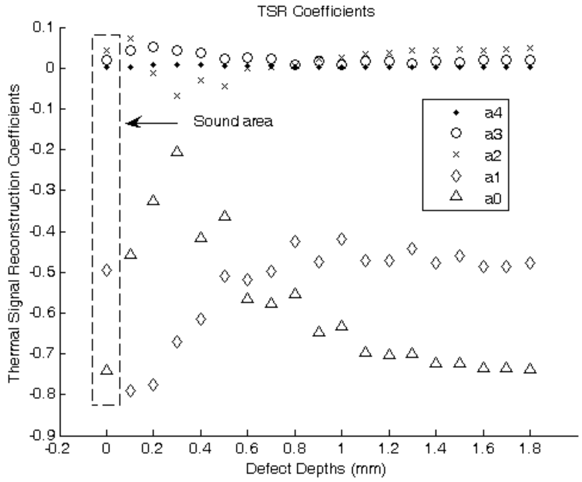

Fig. 2. *TSR coefficients behaviour with respect to defect depth in a CFRP sample*

Simulated composite samples (CFRP) were designed using *ThermoCalc6L* software from *Innovations Inc* [12] in order to analyse the TSR coefficients behaviour with respect to defect depth. For these simulations the TSR coefficients were extracted using a 4th order polynomial from temperature curves over simulated defects (100-μm-thick) that were located at different depths ranging from 0.1 mm to 1.8 mm.. The defect sizes were 16x16 mm^2 to decrease the effects of 3D lateral heat diffusion and follow the behaviour of the 1D transient model described in Eq.(1). As observed in Figure 2, coefficients *a0* and *a1* have the highest sensitivity to depth while coefficients *a2*, *a3* and *a4* present small sensitivity to depth. In addition, the sensitivity decreases for defects deeper than 1 mm. Moreover, for defects with $z < 1$ there is no multivalued output patterns (defect depths), which means that every input pattern (TSR coefficients) represents only one output pattern for these depth range. This conclusion is important because when applying neural networks to inverse problems it is essential to anticipate the possibility that the target data may be multivalued.

2.1 Discrimination ability of TSR coefficients

In ANN applications for classification, it is very important to determine which features (TSR coefficients in this case) preserve the relevant information to use for the training process and architecture selection. To quantitatively determine the discriminating ability of TSR coefficients between defective and non-defective classes we used the lambda Wilks criterion [13] which takes values between 0 and 1, the closer to 0 the higher is the discrimination ability of the selected features.

http://dx.doi.org/10.21611/qirt.2006.010

$$\Lambda_{Wilks} = \frac{|I|}{|I+E|} \qquad (3)$$

Where, *I* is the matrix within groups variability sum of squares and *E* is the matrix between groups variability sum of squares.

Table 1. *Lambda Wilks Criterion*

TSR Coefficients	Discrimination ability
a4	0.936
a3,a4	0.907
a2,a3,a4	0.838
a1,a2,a3,a4	0.780
a0,a1,a2,a3,a4	0.770

Table 1 shows the discriminant ability of TSR coefficients *a0, a1, a2, a3, a4* and some of their combinations; we observe that using the whole set of coefficients provides the most non redundant information.

3. Experimental validation

The network classification ability is evaluated in this section using a 2-mm-thick CFRP sample whose configuration is presented in Figure 3. The locations and geometries of the 25 Teflon® insertions are also indicated in this figure.

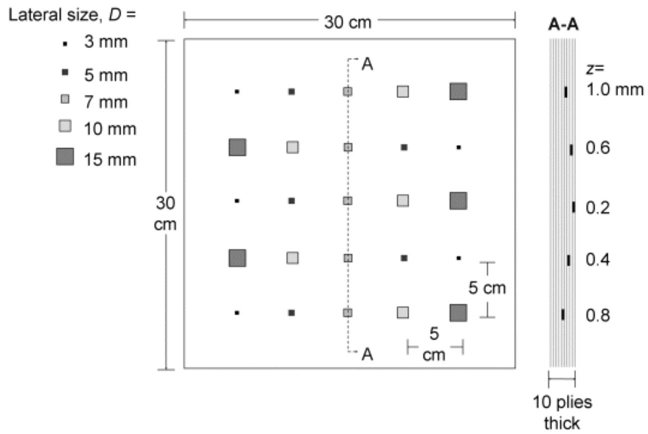

Fig. 3. *CFRP sample with Teflon insertions*

The sampling frequency used to acquire the image sequence for this test is 39.45 Hz and the acquisition time is 6.80 s. For this particular test, only one flash lamp was used as heat source producing a strong non uniform heating pattern. The training set consists of TSR coefficients extracted from experimental temperature curves. These TSR coefficients were obtained by using a 4^{th} order polynomial to fit the temperature curves. In this set, 25 input patterns correspond to defective pixels and 16

http://dx.doi.org/10.21611/qirt.2006.010

correspond to sound pixels. For this test we selected an MLP architecture: 5-10-5 neurons after preliminary test with other architectures and observing that this architecture provides the best performance in terms of correct classified pixels. This network was trained with Bayesian regularization which minimizes a combination of squared errors and weights and then determines the correct combination that produces a network that generalizes well.

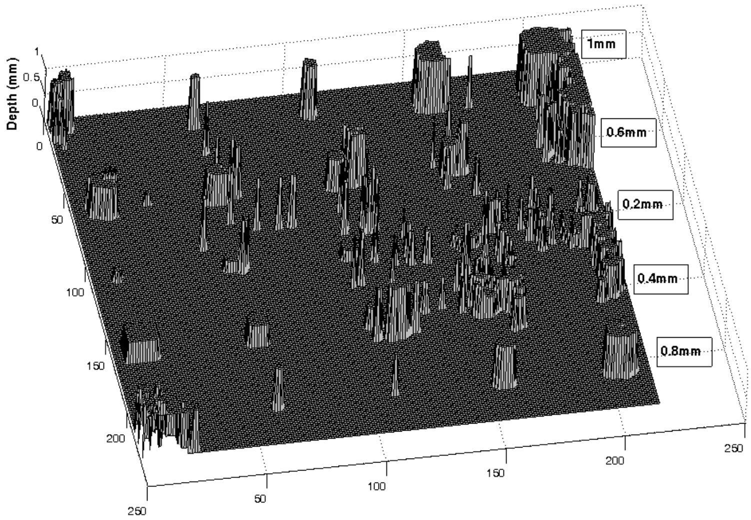

Fig. 4. *ANN output for defect depth estimation in CFRP sample after filtering*

Figure 4 illustrates the ANN output for defect estimation in a CFRP sample after using a 2D median filtering. It is observed that, with the exception of the *z*=0.2 mm defect, all other *D*=3 mm (D is the lateral size) defects were not correctly classified. In addition, false defects detections occur especially in those areas surrounding the smallest defects ($D < 3$ mm) and in the right area which presents a local non-uniform heating. For this test, 80% of defective pixels and 96% of non-defective pixels were correctly classified.

4. Conclusions

The use of ANN to map TSR coefficients into defect depths shows good characterization capabilities. This approach is affected by non-uniform heating since this phenomenon changes the temperature curves so that the least-square fit and TSR coefficients are also influenced and the ANN defect estimation is misled. The TSR coefficients of lowest order (*a0, a1, a2*) present the highest variability with respect to depth and preserves the largest part of information. However, according to the lambda Wilks analysis the higher order coefficients are also important to improve discriminating ability.

5.Acknowlegments

Special acknowledgement for financial support is extended to the Colombian Institute of Science and Technology COLCIENCIAS and Universidad del Valle.

http://dx.doi.org/10.21611/qirt.2006.010

REFERENCES

[1] Carslaw, HS; Jaeger, J C. Conduction of Heat in Solids. Oxford University Press, 2nd edition, (1959)

[2] Shepard, S. Advances in pulsed thermography, *Thermosense XXIII* Proc. SPIE Vol. 5074, Editor Bjorn F. Andresen, Gabor F. Fulop,511-515, (2001)

[3] Shepard, S.; Lhota,J.; Rubadeux, B.; Wang David.; Ahmed T.; Reconstruction and enhancement of active thermography images, *Optical Engineering* 42(5),1337-1342 (2003)

[4] Shepard, S; Hou, Y; Ahmed, T; Lhota, J. Reference-free analysis of flash thermography data, *Thermosense XXVIII Proc. SPIE* Vol. 6205, 352-358;Editor Miles J, Peacock.R, Knettel K (2006)

[5] Shepard,S; Hou,Y; Lhota,J and Ahmed,T. Quantitative Comparison of Thermographic Data Sequences, *Materials Evaluation*. 63 (7) ,740-745 (2005)

[6] Bishop, C. Neural Network and their applications, *Review of Science Instrumentation* 65 (6) (1994)

[7] Darabi, A; Maldague X.Neural Networks Based Detection and Depth Estimation in TNDE. Nondestructive Testing and Evaluation International, 35 [3] ,165-175(2002)

[8] Trétout,H; David,D; Marin, J. Y; Dessendre, M; Couet, M; Avenas-Payan, An evaluation of artificial neural networks applied to infrared thermography inspection of composite aerospace structures, *Review of Progress in Quantitative Nondestructive Evaluation*, Vol 14A, Editor D.O Thompson and D.E Chimenti ,827-834, (1995)

[9] Santey, M.B and Almond, M.B An artificial neural network interpreter for transient thermography data *NDT & E International* Vol 30 (5), 291-295, (1997)

[10] Bison P.G, Marinetti S, Manduchi G, Grinzato E, Improvement of Neural Networks performances in thermal NDE, in *Advances in Signal Processing for Nondestructive Evaluation of Materials*, 3rd Quebec Workshop, Quebec (1998)

[11] Ibarra-Castanedo,C; Avdelidis,N.P; Grinzato,E; Bison, P.G; Marinetti, S; Liu Chen,Genest,M; Maldague,X. Quantitative inspection of non-planar composite specimens by pulsed phase thermography. in press J. QIRT, vol. 3(1) (2006)

[12] Vavilov V – *ThermoCalc* Manual, (2004)

[13] Salvador Figueras, M: "Análisis Discriminante", [On line] *5campus.com, Estadística* <http://www.5campus.com/leccion/discri> [Last access: April 26 2006], (2000).